

Determination of Energetic Positions of Electronic States and the Exciton Dynamics in a π -Expanded *N*-Heterotriangulene Derivative Adsorbed on Au(111)

Jakob Steidel,[†] Ina Michalsky,[‡] Mohsen Ajdari,[†] Milan Kivala,[‡] and Petra
Tegeder^{*,†}

[†]*Ruprecht-Karls-Universität Heidelberg, Physikalisch-Chemisches Institut, Im Neuenheimer
Feld 253, 69120 Heidelberg, Germany*

[‡]*Ruprecht-Karls-Universität Heidelberg, Organisch-Chemisches Institut, Im Neuenheimer
Feld 270, 69120 Heidelberg, Germany*

E-mail: tegeder@uni-heidelberg.de

Phone: +49 (0) 6221 548475

Abstract

Bridged triarylamines, so-called N-heterotriangulenes (N-HTAs) are promising organic semiconductors for applications in optoelectronic devices. Thereby the electronic structure at organic/metal interfaces and within thin films as well as the electronically excited states dynamics after optical excitation is essential for the performance of organic-molecule-based devices. Here, we investigated the energy level alignment and the excited state dynamics of a N-HTA derivative adsorbed on Au(111) by means of energy- and time-resolved two-photon photoemission spectroscopy. We quantitatively determined the energetic positions of several occupied and unoccupied molecular (transport levels) and excitonic states (optical gap) in detail. A transport gap of 3.20 eV and an optical gap of 2.58 eV is determined, resulting in an exciton binding energy of 0.62 eV. With the first time-resolved investigation on a N-HTA compound we gained insights into the exciton dynamics and resolved processes on the femtosecond to picosecond timescale.

N-heteropolycyclic aromatic compounds represent a promising molecule class for applications in functional organic materials, since their electronic structure and the resulting individual molecular properties are efficiently tuneable by number and position of nitrogen atoms in the aromatic structural backbone. The isosteric replacement of a C–H unit by N leaves the geometric structure unchanged, while the electronic structure are altered. For instance, they are promising candidates for electron-transporting (n-channel) semiconductors, which are of great interest for organic field effect transistors.^{1–5} N-heterotriangulenes (N-HTAs), in which the originally propeller-shaped triphenylamine unit is locked into a planar configuration via bridging with appropriate molecular moieties (e.g. carbonyl or dimethylmethylene)^{6–8} is a class of functional molecules with high potential for optoelectronic materials.^{9–12} In electron donor/acceptor systems N-HTAs act as the donor compound.¹³ Recently, we analyzed the electronic and absorption properties of two N-HTA derivatives (N-HTA-550 and N-HTA-557, see Fig. 1) at the interface to Au(111) and within thin molecular films using vibrational and electronic high resolution electron energy loss spectroscopy and quantum chemical calcula-

tions. Inter alia, we found that the additional -C=C- bridge forming the 7-membered ring in N-HTA-557 resulted in a pronounced reduction of the optical gap size by 0.9 eV from 3.4 eV in N-HTA-550 to 2.5 eV in N-HTA-557 due to an increase of the π -conjugated electron system.¹⁴ Thus, using structural extensions or substitution patterns opens the opportunity for fine-tuning the electronic properties.^{7,10,15} Here, we investigated the electronic structure and electronically excited state dynamics of a novel π -expanded N-heterotriangulene derivative (N-HTA-557-P, see Fig. 1), which consists of an electron-deficient pyrazine ring (electron accepting unit)⁷ adsorbed on Au(111) utilizing two-photon photoemission (2PPE) spectroscopy. 2PPE has been proven to be a powerful tool, which provides the unique op-

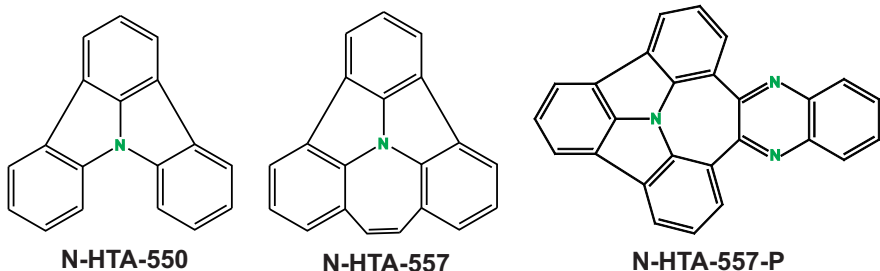


Figure 1: The N-heterotriangulenes N-HTA-550 and N-HTA-557. The π -expanded derivative N-HTA-557-P investigated in the present study.

portunity for a quantitative determination of the energetic position of occupied as well as unoccupied molecular electronic states (transport levels) but also excitonic states (optical gaps) and therefore exciton binding energies.^{16–34} In addition, femtosecond (fs) time-resolved 2PPE allows to gain insights into the electronically excited states dynamics after optical excitation such as exciton formation and decay dynamics.

Here we thoroughly elucidated the electronic structure of N-HTA-557-P/Au(111) in detail, including the determination of transport levels, the optical gap and accordingly the exciton binding energy. In particular for applications of this material in organic field effect transistors or solar cells knowledge about the energetic positions of transport levels (affinity levels and ionization potentials) are extremely important. Moreover, fs-time-resolved 2PPE, allowed to gain insights into the exciton dynamics. Our study represents the first time-

resolved investigation on a N-HTA-derived compound, which is of great interest with respect to applications of this donor material in organic solar cells.

To gain insight into the energy level alignment, i.e., the energetic positions of adsorbate-derived occupied as well as unoccupied electronic states we conducted photon-energy-dependent 2PPE measurements.^{23–26,30–33,35} Figure 2a shows an exemplarily 2PPE spectrum of 5 monolayer (ML) N-HTA-557-P adsorbed on Au(111) recorded with $h\nu = 4.62$ eV (for additional 2PPE data see supporting information). Several photoemission features could be detected. On the basis of their photon-energy-dependency they are assigned to occupied and unoccupied molecular orbitals as well as an excitonic state (see Fig. 2b).

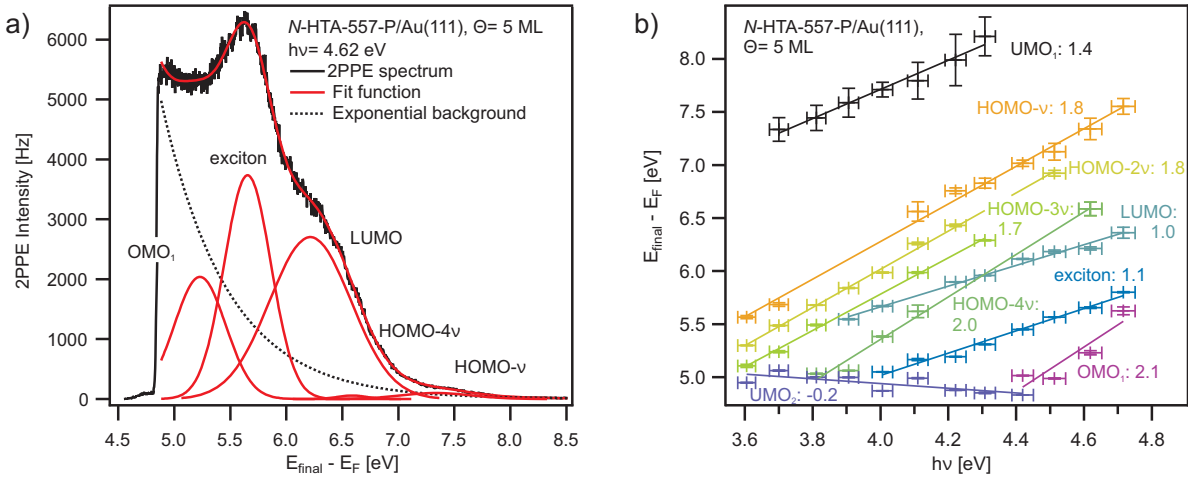


Figure 2: a) 2PPE spectrum of 5 monolayer (ML) N-HTA-557-P adsorbed on Au(111). The data are fitted with an exponential background and Gaussian-shaped peaks (red curves). The energy axis reveals the final state (E_{Final}) of photoemitted electrons with respect to the Fermi energy E_F ($E_{Final} - E_F = E_{kin} + \Phi$); thus, the low-energy cutoff corresponds to the work function (Φ) of the adsorbate/substrate system. b) Photon-energy-dependent peak position extracted to assign peaks observed in the 2PPE spectrum to occupied, unoccupied intermediate or final electronic states. A slope of 1 suggests that a peak originates from an unoccupied intermediate state, a slope of zero from an unoccupied final state (located above the vacuum level), while a slope of 2 is related to peaks originating from occupied states. The slopes from the fits are given next to the respective data.

In Figure 3, we summarize the level alignments with respect to the vacuum level. Note that the work function of bare Au(111) ($\Phi_{Au(111)} = 5.5$ eV) decreases by 0.7 eV due to the adsorption of 1 ML N-HTA-557-P (see supporting information, Figs. S1 and S2) and

stays constant for higher coverages. As discussed before,^{24,25,30,36,37} depending on the excitation mechanism 2PPE probes transport levels. Unoccupied single-electron states can be

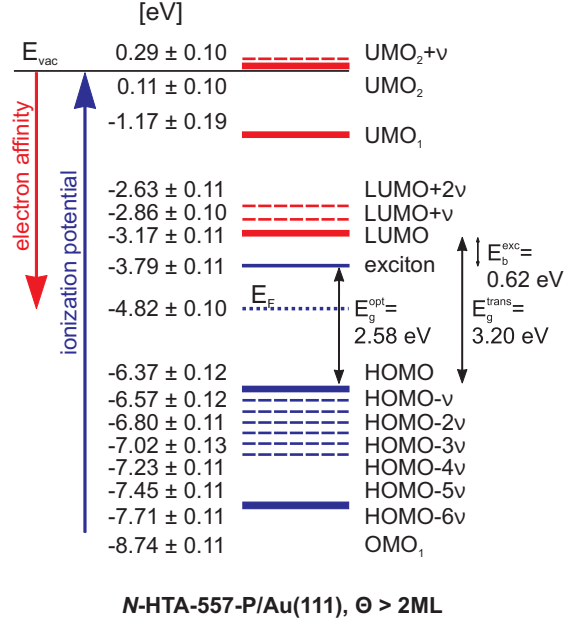


Figure 3: Energy level diagram of N-HTA-557-P adsorbed on Au(111) for N-HTA-557-P coverages above 2 ML with respect to the vacuum level. The blue levels are the ionization potentials and the red ones are the electron affinities, which are in the molecular orbital picture represented by the energies of the HOMO, LUMO, UMOs (unoccupied molecular orbital) or OMO (occupied molecular orbital), respectively. The dashed lines indicate vibronic transition. E_F is the Au(111) Fermi level.

populated via an electron transfer from the metal to the N-HTA-557-P molecule creating a negative ion resonance and occupied single-electron states are ionized, creating a positive ion resonance. Thus, we obtain the electron affinities (EA) and the ionization potentials (IP) of the investigated molecule. In addition, in 2PPE also intramolecular electronic excitation is possible, which corresponds to exciton generation, i.e. formation of an electron-hole pair, in which the molecule remains overall neutral. The minimal energy required for this process is the optical gap (E_{opt}), which corresponds to the excitation energy of the lowest excited singlet state. E_{opt} is smaller than the difference between the lowest IP and the highest EA. The so-called transport gap is given as $E_{transp} = IP - EA$. The difference between the transport gap and the optical gap corresponds to the exciton binding energy $E_{transp} - E_{opt} = E_B$.^{19,38} For the N-HTA-557-P we obtain a transport gap of 3.20 eV ($IP = 6.37$ eV, $EA = 3.17$

eV), and an optical gap of 2.58 eV, the excitation energy of the lowest excited singlet state. Hence, the exciton binding energy (E_B) of this lowest excitonic state amounts to 620 meV. For comparison, N-HTA-557-P in solution (CH_2Cl_2) possesses an optical gap of 2.61 eV (see supporting information, Fig. S3). The similar value indicates that the adsorbed molecules (5 ML) are decoupled from the metallic substrate and weak adsorbate-adsorbate (lateral) interactions. In addition, we identified two further unoccupied molecular states (unoccupied molecular orbital: UMO), an intermediate (at 1.17 eV) and a final state (0.11 eV above E_{vac}) as well as an occupied molecular state (occupied molecular orbital: OMO) at 8.74 eV. All other 2PPE features are assigned to vibronic contributions related to the LUMO, and UMO_2 as well as to the HOMO. They exhibit an equidistance energy different of around 200 meV, which can be related to an excitation of $\nu(\text{C-C})$ and $\delta(\text{C-H})$ vibrational modes of the N-HTA-557 moiety of N-HTA-557-P located at 1636 cm^{-1} (see supporting information Fig. S4 and Tab. S1). Vibronic features in 2PPE data have recently been also proposed for another N-heterocyclic compound adsorbed on Au(111) supported by scanning tunneling spectroscopy results.³³ For lower N-HTA-557-P coverages, i.e., around 1ML contributions from the Au(111) surface, the d -bands, the shifted surface state and the first image potential state are visible in the 2PPE data (see supporting information, Fig. S1).

We used femtosecond time-resolved 2PPE to study how the electronic coupling between the N-HTA-557-P molecules and the metal substrate influences the dynamics of optically excited states such as excitons in N-HTA-557-P. For low coverages (1–2 ML) none of the electronically excited states, e.g. the LUMO or excitonic states, exhibit a detectable lifetime, thus $\tau < 10\text{ fs}$. The reason for these ultrashort lifetimes is a strong electron coupling enabling an efficient electron transfer from the molecule back to the metal. Such short lifetime in the order of a few femtoseconds have been found also for other adsorbates on metal surfaces.^{35,39–41} In contrast, for higher coverages longer lifetimes are usually observed. This is the case for our findings as can be seen Fig. 4a for 15 ML N-HTA-557-P on Au(111) in a two-dimensional false colored plot representation taken at a pump photon energy of

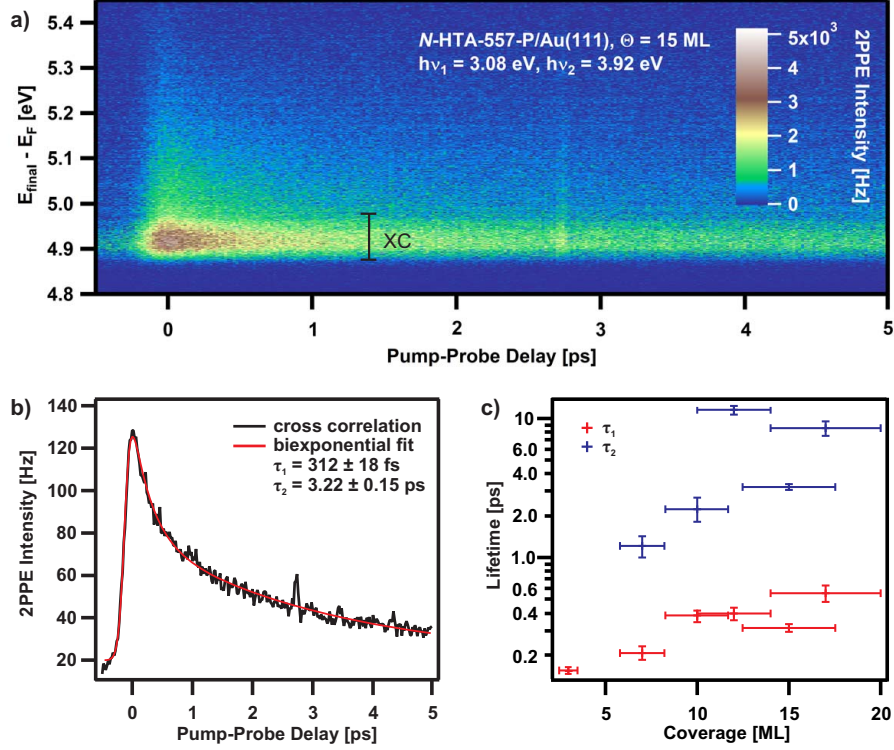


Figure 4: a) 2D-plot of the 2PPE intensity as a function of final-state energy and the pump-probe delay for 15 ML N-HTA-557-P on Au(111). b) The cross-correlation (XC) curves fitted by a sech^2 function convoluted by a double exponential decay (XC energy range in a)). c) Coverage dependent lifetimes.

$h\nu_1 = 3.08$ eV and a probe photon energy $h\nu_2 = 3.92$ eV. Such representations visualize the normalized correlated dichromatic 2PPE signal at a given final state energy (E_{Final}) with respect to E_F as a function of pump-probe delay. Positive pump-probe delays imply that the pump pulse $h\nu_1$ reaches the sample after the probe pulse $h\nu_2$, and *vice versa* for negative delays. A long-lived contribution can clearly be seen in the energy region around 4.9 eV, thus the energy at which we identified the first excitonic state. To receive the lifetimes of the involved state a cross-correlation (XC) curve as shown in Fig. 4b has been employed. To fit the XC curve, we used a sech^2 -function representing the laser pulse duration convoluted with a response function of the intermediate state. A superposition of two exponential decays with different time constants, τ_1 and τ_2 , describes the time-resolved photoemission data well (see solid line in Fig. 4 b)). The time constants are $\tau_1 = 312 \pm 18$ fs and $\tau_2 = 3.22 \pm 0.15$ ps at a

coverage of 15 ML. Coverage-dependent measurements (see Fig.4c) clearly demonstrate that the lifetimes increase with rising coverage. Coverage-dependent lifetimes can be explained by the availability of two relaxation channels.^{24–26,40,42} An intrinsic channel due to the decay in the bulk material and a distance-dependent (external) channel resulting from a quenching process by the metallic substrate, i.e, transfer of the electrons to the metal. Note that, in literature no time-dependent measurements on the N-HTAs excited states dynamics are available. However, by comparing with our previous time-resolved 2PPE results obtained from other electron donating materials^{24,25} we consider the following processes: Excitation with a photon energy of 3.08 eV leads to the creation of hot ($E_{opt.} = 2.58\text{eV}$), delocalized excitons. These excitons relax and localize on an ultrafast time-scale ($\tau_1 = 312\pm 18$ fs). A very fast relaxation of hot excitons has also been found in other organic semiconductors.^{43–46} The longer lived component ($\tau_2 = 3.22\pm 0.15$ ps) may be related to the decay of the exciton to the ground state. However, it could also be connected to the lifetime of polarons as well as electrons bound at defect sites. Note, that no energetic stabilization is observed, which would be expected for polaron formation or population of defect sites.

In summary, we employed energy- and time-resolved two-photon photoemission spectroscopy to quantitatively determine the energetic positions of unoccupied and occupied electronic states as well as an excitonic state and to resolve the exciton dynamics in a novel π -expanded N-heterotriangulene derivative adsorbed on Au(111). A transport gap of 3.20 eV and an optical gap of 2.58 eV have been identified, resulting in an exciton binding energy of 0.62 eV. Hot and delocalized excitons have found to localize on a femtosecond timescale followed by an exciton decay within picoseconds. The quantitative determination of the energetic positions of molecular electronic levels, the achieved detailed understanding of the electronic structure and insights into the exciton dynamics is an essential prerequisite for the design of new functional organic molecules for (opto)electronic devices.

Experimental Methods

2PPE measurements were conducted in an ultra-high vacuum chamber. A clean Au(111) substrate was prepared by a standard procedure including Ar⁺ sputtering and subsequent annealing to 800 K under ultra-high vacuum conditions. The N-HTA-557-P molecules were synthesized according to Ref.,⁷ purified by column chromatography and degassed in vacuum at 400 K for several hours. They were deposited from an effusion cell held at a temperature of 453 K while the surface was kept at 100 K. The experiments were performed at a sample temperature of around 90 K. In 2PPE, a femtosecond pump laser pulse induces electronic transitions from occupied electronic states of the substrate or the adsorbate into unoccupied electronic or virtual states. These excited states are then probed with a second laser pulse by lifting the excited electron above the vacuum level. The kinetic energy of the emitted electrons is measured with a time-of-flight spectrometer. Photoelectron signals may arise from the occupied or unoccupied electronic states; therefore, photon energy-dependent measurements are needed for the assignment (for details, see refs see^{24,25,47}). A temporal delay between pump and probe pulse was introduced to obtain population dynamics of excited states on a femtosecond time scale.^{24,42}

Acknowledgement

Funding by the German Research Foundation (DFG) through the collaborative research center SFB 1249 "N-Heteropolycycles as Functional Materials" (Project Number 281029004-SFB 1249, projects A05 and B06) is gratefully acknowledged.

Supporting Information Available

Two-photon photoemission data, UV/vis absorption and emission data as well as infrared vibrational data.

References

- (1) Klauk, H.; Zschieschang, U.; Pflaum, J.; Halik, M. Ultralow-Power Organic Complementary Circuits. *Nature* **2007**, *445*, 745–748.
- (2) Würthner, F.; Stolte, M. Naphthalene and Perylene Diimides for Organic Transistors. *Chem. Commun.* **2011**, *47*, 5109–5115.
- (3) Bunz, U. H. F.; Engelhart, J. U.; Lindner, B. D.; Schaffroth, M. Large N-Heteroacenes: New Tricks for Very Old Dogs? *Angew. Chem. Int. Ed.* **2013**, *52*, 3810–3821.
- (4) Miao, Q. Ten Years of N-Heteropentacenes as Semiconductors for Organic Thin-Film Transistors. *Adv. Mater.* **2014**, *26*, 5541–5549.
- (5) Bunz, U. H. F. The Larger Linear N-Heteroacenes. *Acc. Chem. Res.* **2015**, *48*, 1676–1686.
- (6) Hammer, N.; Schaub, T. A.; Meinhardt, U.; Kivala, M. N-Heterotriangulenes: Fascinating Relatives of Triphenylamine. *Chem. Rec.* **2015**, *15*, 1119–1131.
- (7) Michalsky, I.; Gensch, V.; Walla, C.; Hoffmann, M.; Rominger, F.; Oeser, T.; Tegeder, P.; Dreuw, A.; Kivala, M. Fully Bridged Triphenylamines Comprising Five- and Seven-Membered Rings. *Chem. Eur. J.* **2022**, *28*, e202200326.
- (8) Wagner, J.; Crocomo, P. Z.; Kochman, M. A.; Kubas, A.; Data, P.; Lindner, M. Modular Nitrogen-Doped Concave Polycyclic Aromatic Hydrocarbons for High-Performance Organic Light-Emitting Diodes with Tunable Emission Mechanisms. *Angew. Chem. Int. Ed.* **2022**, *61*, e202202232.
- (9) Meinhardt, U.; Lodermeier, F.; Schaub, T. A.; Kunzmann, A.; Dral, P. O.; Sale, A. C.; Hampel, F.; Guldi, D. M.; Costa, R. D.; Kivala, M. N-Heterotriangulene Chromophores with 4-Pyridyl Anchors for Dye-Sensitized Solar Cells. *RSC Adv.* **2016**, *6*, 67372–67377.

- (10) Hirai, M.; Tanaka, N.; Sakai, M.; Yamaguchi, S. Structurally Constrained Boron-, Nitrogen-, Silicon-, and Phosphorus-Centered Polycyclic π -Conjugated Systems. *Chem. Rev.* **2019**, *119*, 8291–8331.
- (11) Schaub, T. A.; Padberg, K.; Kivala, M. Bridged Triarylboranes, -Silanes, -Amines, and -Phosphines as Minimalistic Heteroatom-Containing Polycyclic Aromatic Hydrocarbons: Progress and Challenges. *J. Phys. Org. Chem.* **2020**, *33*, e4022.
- (12) Krug, M.; Wagner, M.; Schaub, T. A.; Zhang, W.; Schüßlbauer, C. M.; Ascherl, J. D. R.; Münich, P. W.; Schröder, R. R.; Gröhn, F.; Dral, P. O.; et al., Quantification of a CH- π Interaction Responsible for Chiral Discrimination and Evaluation of Its Contribution to Enantioselectivity. *Angew. Chem. Int. Ed.* **2020**, *59*, 16233–16240.
- (13) Kader, T.; Stöger, B.; Fröhlich, J.; Kautny, P. Azaindolo[3,2,1-jk]carbazoles: New Building Blocks for Functional Organic Materials. *Chem. Eur. J.* **2019**, *25*, 4412–4425.
- (14) Ajdari, M.; Pappenberger, R.; Walla, C.; Hoffmann, M.; Michalsky, I.; Kivala, M.; Dreuw, A.; Tegeder, P. The Impact of Connectivity on the Electronic Structure of N-Heterotriangulenes. *J. Phys. Chem. C* **2023**, *127*, 542–549.
- (15) Deng, N.; Zhang, G. Nitrogen-Centered Concave Molecules with Double Fused Pentagons. *Org. Lett.* **2019**, *21*, 5248–5251.
- (16) Zhu, X.-Y. Electronic Structure and Electron Dynamics at Molecule-Metal Interfaces: Implications for Molecule-Based Electronics. *Surf. Sci. Rep.* **2004**, *56*, 1–83.
- (17) Zhu, X.-Y. Charge Transport at Metal-Molecule Interfaces: A Spectroscopic View. *J. Phys. Chem. B* **2004**, *108*, 8778–8793.
- (18) Lindstrom, C.; Zhu, X.-Y. Photoinduced Electron Transfer at Molecule-Metal Interfaces. *Chem. Rev.* **2006**, *106*, 4281–4300.

- (19) Muntwiler, M.; Zhu, X.-Y. In *Dynamics at Solid State Surfaces and Interfaces*; Boven-siepen, U., Petek, H., Wolf, M., Eds.; Wiley-VCH, 2010.
- (20) Bronner, C.; Schulze, M.; Hagen, S.; Tegeder, P. The Influence of the Electronic Structure of Adsorbate–Substrate Complexes on Photoisomerization Ability. *New J. Phys.* **2012**, *14*, 043023.
- (21) Bronner, C.; Schulze, G.; Franke, K. J.; Pascual, J. I.; Tegeder, P. Switching Ability of Nitro-Spiropyran on Au(111): Electronic Structure Changes as a Sensitive Probe During a Ring-Opening Reaction. *J. Phys.: Condens. Matter* **2011**, *23*, 484005.
- (22) Armbrust, N.; Gddde, J.; Jakob, P.; Hfer, U. Time-Resolved Two-Photon Photoemission of Unoccupied Electronic States of Periodically Rippled Graphene on Ru(0001). *Phys. Rev. Lett.* **2012**, *108*, 056801.
- (23) Bronner, C.; Stremlau, S.; Gille, M.; Braue, F.; Haase, A.; Hecht, S.; Tegeder, P. Aligning the Band Gap of Graphene Nanoribbons by Monomer Doping. *Angew. Chem. Int. Ed.* **2013**, *52*, 4422–4425.
- (24) Bogner, L.; Yang, Z.; Baum, S.; M. Corso, R. F.; Buerle, P.; Franke, K. J.; Pascual, J. I.; Tegeder, P. Electronic States and Exciton Dynamics in Dicyanovinyl-Sexithiophene on Au(111). *J. Phys. Chem. C* **2016**, *120*, 27268–27275.
- (25) Bogner, L.; Yang, Z.; Corso, M.; Fitzner, R.; Buerle, P.; Franke, K. J.; Pascual, J. I.; Tegeder, P. Electronic Structure and Excited States Dynamics in a Dicyanovinyl-Substituted Oligothiophene on Au(111). *Phys. Chem. Chem. Phys.* **2015**, *17*, 27118–27126.
- (26) Stein, A.; Maass, F.; Tegeder, P. Triisopropylsilylethynyl-Pentacene on Au(111): Adsorption Properties, Electronic Structure and Singlet-Fission Dynamics. *J. Phys. Chem. C* **2017**, *121*, 18075–18083.

- (27) Gerbert, D.; Maass, F.; Tegeder, P. Extended Space Charge Region and Unoccupied Molecular Band Formation in Epitaxial Tetrafluoro-tetracyanoquinodimethane Films. *J. Phys. Chem. C* **2017**, *121*, 15696–15701.
- (28) Gerbert, D.; Tegeder, P. Molecular Ion Formation by Photo-Induced Electron Transfer at the Tetracyanoquinodimethane/Au(111) Interface. *J. Phys. Chem. Lett.* **2017**, *8*, 4685–4690.
- (29) Bronsch, W.; Wagner, T.; Baum, S.; Wansleben, M.; Zielke, K.; Ghanbari, E.; Györök, M.; Navarro-Quezada, A.; Zeppenfeld, P.; Weinelt, M.; et al., Interplay between Morphology and Electronic Structure in Sexithiophene Films on Au(111). *J. Phys. Chem. C* **2019**, *123*, 7931–7939.
- (30) Stein, A.; Rolf, D.; Lotze, C.; Czekelius, C.; Franke, K. J.; Tegeder, P. Electronic Structure of an Iron-Porphyrin Derivative on Au(111). *J. Phys.: Condens Matter* **2019**, *31*, 044002.
- (31) Ajdari, M.; Stein, A.; Hoffmann, M.; Müller, M.; Bunz, U. H. F.; Dreuw, A.; Tegeder, P. Lightening up a Dark State of a Pentacene Derivative via N-Introduction. *J. Phys. Chem. C* **2020**, *124*, 7196–7204.
- (32) Stein, A.; Rolf, D.; Lotze, C.; Günther, B.; Gade, L. H.; Franke, K. J.; Tegeder, P. Band Formation at Interfaces Between N-Heteropolycycles and Gold Electrodes. *J. Phys. Chem. Lett.* **2021**, *12*, 947–951.
- (33) Stein, A.; Rolf, D.; Lotze, C.; Feldmann, S.; Gerbert, D.; Günther, B.; Jeindl, A.; Caratus, J. J.; Hofmann, O. T.; Gade, L. H.; et al., Electronic Properties of Tetraazaperopyrene Derivatives on Au(111): Energy Level Alignment and Interfacial Band Formation. *J. Phys. Chem. C* **2021**, *125*, 19969–19979.
- (34) Stallberg, K.; Namgalies, A.; Chatterjee, S.; Höfer, U. Ultrafast Exciton Dynamics and

- Charge Transfer at PTCDA/Metal Interfaces. *J. Phys. Chem. C* **2022**, *126*, 12728–12734.
- (35) Bronner, C.; Schulze, M.; Hagen, S.; Tegeder, P. The Influence of the Electronic Structure of Adsorbate-Substrate Complexes on the Photoisomerization Ability. *New J. Phys.* **2012**, *14*, 043032.
- (36) Varene, E.; Martin, I.; Tegeder, P. Optically Induced Inter- and Intrafacial Electron Transfer Probed by Two-Photon Photoemission: Electronic States of Sexithiophene on Au(111). *J. Phys. Chem. Lett.* **2011**, *2*, 252–256.
- (37) Bronner, C.; Gerbert, D.; Broska, A.; Tegeder, P. Excitonic States in Narrow Armchair Graphene Nanoribbons on Gold Surfaces. *J. Phys. Chem. C* **2016**, *120*, 26168–26172.
- (38) Knupfer, M. Exciton Binding Energies in Organic Semiconductors. *Appl. Phys. A* **2003**, *77*, 623–626.
- (39) Yang, A.; Shipman, S. T.; Garrett-Roe, S.; Johns, J.; Strader, M.; Szymanski, P.; Muller, E.; Harris, C. B. Two-Photon Photoemission of Ultrathin Film PTCDA Morphologies on Ag(111). *J. Phys. Chem. C* **2008**, *112*, 2506.
- (40) Dutton, G.; Quinn, D. P.; Lindstrom, C. D.; Zhu, X.-Y. Exciton Dynamics at Molecule-Metal Interfaces: C60 /Au(111). *Phys. Rev. B* **2005**, *72*, 045441.
- (41) Hagen, S.; Luo, Y.; Haag, R.; Wolf, M.; Tegeder, P. Electronic Structure and Electron Dynamics at an Organic Molecule/Metal Interface: Interface States of tetra-tert-butyl-Imine/Au(111). *New J. Phys.* **2010**, *12*, 125022 (17pp).
- (42) Varene, E.; Bogner, L.; Bronner, C.; Tegeder, P. Ultrafast Exciton Population, Relaxation, and Decay Dynamics in Thin Oligothiophene Films. *Phys. Rev. Lett.* **2012**, *109*, 7601–1.

- (43) Marks, M.; Sachs, S.; Schwalb, C.; Schöll, A.; Höfer, U. Electronic Structure and Excited State Dynamics in Optically Excited PTCDA Films Investigated with Two-Photon Photoemission. *J. Chem. Phys.* **2013**, *139*, 124701.
- (44) Engel, E.; Koschorreck, M.; Leo, K.; Hoffmann, M. Ultrafast Relaxation in Quasi-One-Dimensional Organic Molecular Crystals. *Phys. Rev. Lett.* **2005**, *95*, 157403.
- (45) Guo, J.; Ohkita, H.; Bente, H.; Ito, S. Near-IR Femtosecond Transient Absorption Spectroscopy of Ultrafast Polaron and Triplet Exciton Formation in Polythiophene Films with Different Regioregularities. *J. Am. Chem. Soc.* **2009**, *131*, 16869–16880.
- (46) Chen, K.; Barker, A.; Reish, M.; Gordon, K.; Hodgkiss, J. M. Broadband Ultrafast Photoluminescence Spectroscopy Resolves Charge Photogeneration via Delocalized Hot Excitons in Polymer: Fullerene Photovoltaic Blends. *J. Am. Chem. Soc.* **2013**, *135*, 18502–18512.
- (47) Tegeder, P. Optically and Thermally Induced Molecular Switching Processes at Metal Surfaces. *J. Phys.: Condens. Matter* **2012**, *24*, 394001 (34pp).